



**HAL**  
open science

# Design Optimization of Polyarticulated Robot for SEM Micromanipulation

Spiro Dourbaly, Kanty Rabenorosoa, Jean-Yves Rauch, Cédric Clevy

► **To cite this version:**

Spiro Dourbaly, Kanty Rabenorosoa, Jean-Yves Rauch, Cédric Clevy. Design Optimization of Polyarticulated Robot for SEM Micromanipulation. International Conference on Manipulation, Automation and Robotics at Small Scales, Jul 2024, Delft, Netherlands. 10.1109/MARSS61851.2024.10612707 . hal-04692803

**HAL Id: hal-04692803**

**<https://hal.science/hal-04692803>**

Submitted on 10 Sep 2024

**HAL** is a multi-disciplinary open access archive for the deposit and dissemination of scientific research documents, whether they are published or not. The documents may come from teaching and research institutions in France or abroad, or from public or private research centers.

L'archive ouverte pluridisciplinaire **HAL**, est destinée au dépôt et à la diffusion de documents scientifiques de niveau recherche, publiés ou non, émanant des établissements d'enseignement et de recherche français ou étrangers, des laboratoires publics ou privés.

# Design Optimization of Polyarticulated Robot for SEM Micromanipulation

Spiro Dourbaly<sup>1</sup>, Kanty Rabenoroso<sup>1</sup>, Jean-Yves Rauch<sup>1</sup> and Cédric Clévy<sup>1</sup>

**Abstract**— This paper introduces an approach to optimize the design of serial robots tailored to achieve tasks within confined spaces such that of a Scanning Electron Microscope (SEM). Given the available working area, where tasks and visualization are restricted to a very small volume (few  $1\text{mm}^3$ ), numerous systems revolve around this limited space, constraining the area available for integrating a manipulation robot. To address this challenge, we aim to optimize the robotic structure’s design, making it more compact and closer to the area of interest, thereby enhancing the workspace. The primary objective of the optimization process is to maximize the robot’s capability to attain significant angular orientations that currently drastically limits manipulation abilities and accessibility of the robots. The proposed methodology provides systematic means to address the challenges posed by the constrained environment, ensuring the serial robot’s work performance within the SEM. The resulting robot architecture meets the criteria of large workspace and the ability to achieve a large angular rotation of  $34^\circ$  which is more than double the largest rotation of the actual robot using the same stages, thereby enhancing the overall capabilities of serial robots for SEM applications.

## I. INTRODUCTION

Robot design optimization techniques find application in diverse fields, including surgical robotics [1], robotic manipulation [2], and industrial robots [3]. These techniques are primarily employed to tackle challenges associated with reducing robot mass, enhancing cost-effectiveness, and optimizing robot placement. Various approaches are utilised, such as heuristic optimization algorithms [2], [4], gradient based optimization algorithms [5] and analytical methods [6]. However, to our knowledge, no works have been made in the literature concerning the optimization of robot workspace within confined environments as shown in **Figure 1**. This article aims to fill this research gap by addressing the specific challenges associated with robot workspace optimization in constrained spaces, and more especially under powerful microscopes.

In this article, a case study of robot kinematic optimization for SEM (Scanning Electron Microscope) micro manipulation is proposed. The SEM is a potent tool for high-resolution specimen imaging in a vacuum environment. Systems are included in the chamber such as a Focused Ion Beam (FIB) and Gas Injection System (GIS) for subtractive and additive micro manufacturing, a SESI detector to capture secondary electrons for image generation as well as a 5 DOF sample stage for sample positioning. It can be noticed from **Figure**

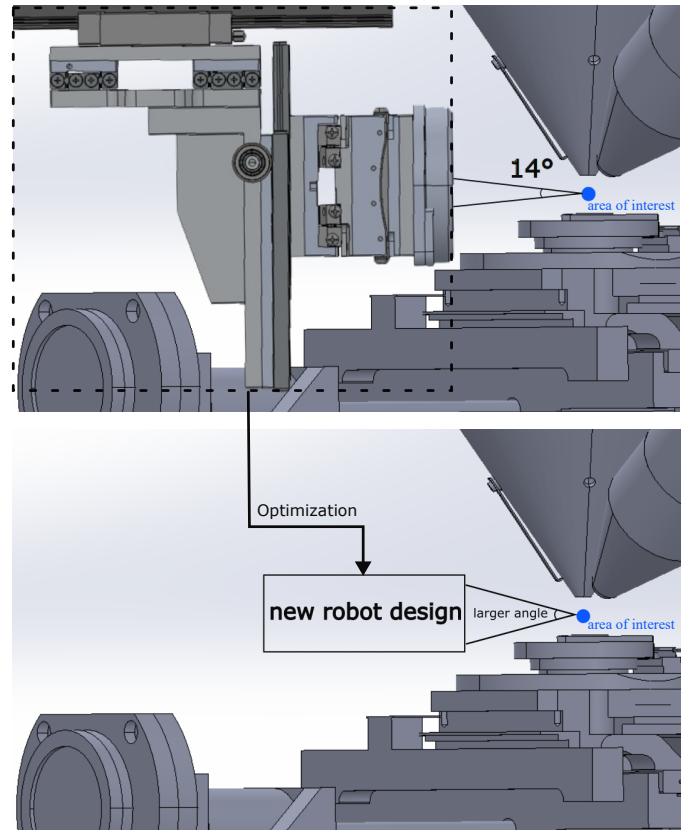


Fig. 1. Robot limited rotation around the area of interest due to confined space

2 that all systems within the SEM revolve around the electron gun column, hence a vertical plane passing through the electron gun is considered for the optimization process.

Commercially available positioners capable of nanometric repeatability could be mounted in series to form a serial robot manipulator are increasingly used in the vacuum chamber. This research unveils the integration of advanced robotic systems to enhance micro-scale operations in SEM applications. A number of teams used these nanopositioning robots in SEM to achieve robotic tasks such as cell characterization [7], nano manipulation [8] and nano-assembly [9].

The robot employed within the SEM, as depicted in **Figure 3** is utilized for diverse tasks, including the fabrication of lab-on fiber 3D structures [10], characterisation of microscale particles [11], creating a large workspace silica structure [12] and fabrication of folding micro gripper [13]. These tasks are strategically performed at the intersection of the field of view

<sup>1</sup> FEMTO-ST Institute, Université de Franche-Comté, SUPMICROTECH-ENSMM, CNRS, 25000 Besançon, France spiro.dourbaly@femto-st.fr, cedric.cleavy@femto-st.fr

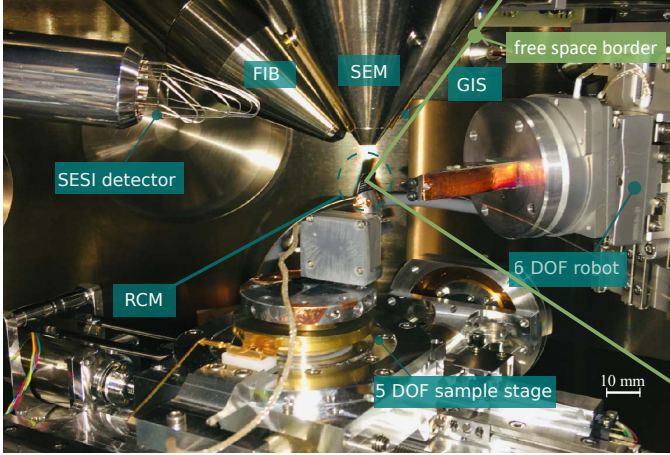


Fig. 2. View of the SEM vacuum chamber showing the limited free space for robot integration in addition to area of interest on FIB/SEM

of the electron gun and the FIB, forming an area of interest, the Remote Center of Motion (RCM). The free space where the robot is mounted and operate in is shown in **Figure 2**, as the RCM is at the tip of the conical volume, installing nano positioners near the point of interest is not feasible due to their bulky size (in the order of tens of cm), which forces the base of the robot to be mounted far from the RCM. This leads to the robot facing limitations in executing substantial movement around this point, especially in rotations, that are essential in accomplishing robotic tasks (a maximum of  $14^\circ$  in the XY), attributed to the restrictive and narrow inner geometry of the electron microscope, and to the inherent architecture of the robot that doesn't consider the point of interest, resulting in a reduction in the manipulation ability of the robot. To overcome this challenge, we propose an optimization approach aimed at changing the robotic design to attain a larger working angle.

The envisioned design aims to achieve two key objectives:

(a) Enable large rotations around the RCM. In micro manipulation, achieving significant rotations is crucial for achieving robotic tasks, since this amelioration will result an increase in robot workspace, dexterity and manipulability.

(b) Ensure collision-free navigation within the SEM vacuum environment to prevent any incidents.

Addressing this challenge involved a series of strategic actions: Section II will introduce the kinematic modeling of the robots and the consideration of geometrical free space limitations in the microscope. Section III will provide a passage on configuration free space estimation to be used in section IV that consists in the identification of the parameters conducting to the optimal robot design. Section V provides the final results as well as future perspective.

## II. KINEMATIC MODELLING OF THE ROBOT AND SEM ENVIRONMENT

In this section, the means for calculating the largest angle possible around the area of interest without collision with the

SEM environment are going to be introduced. To achieve this feat, a model to describe the kinematics of the robot and the SEM environment will be presented.

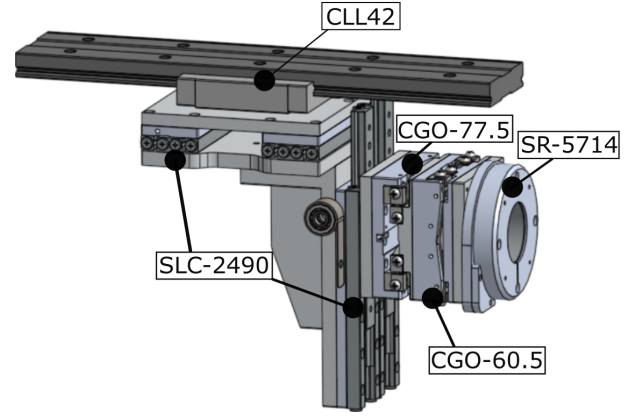


Fig. 3. CAD model of the current 6 DOF robot inside the SEM

### A. Robot kinematic modelling

For the scope of this study, a 2D,  $XY\theta$  structure was considered, this is due to the consideration that the SEM is axisymmetric; as all systems in the SEM revolve around the electron column. We considered the linear X, Y actuators and the rotational  $\theta$  (around Z) stage from the original robot. The frames describing the robotic structure with a tool of length  $L$  can be obtained as shown in **Figure 4**:

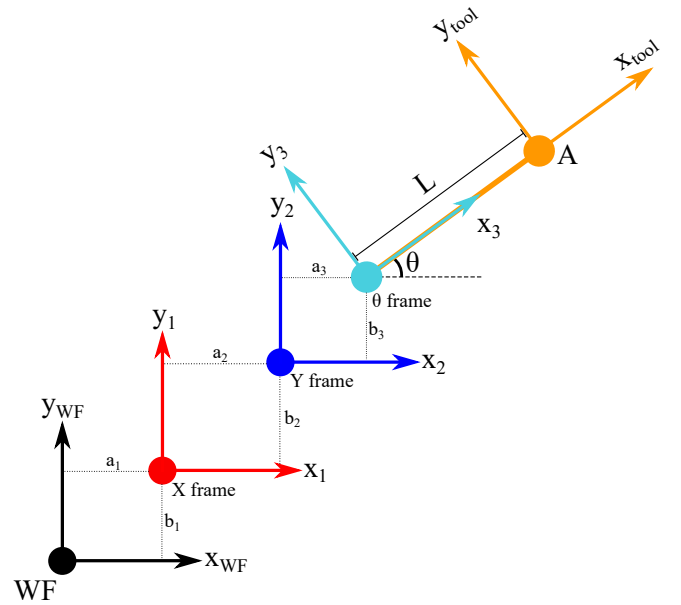


Fig. 4. Kinematic model of a  $XY\theta$  robot

For  $i \leq 3$ ,  $(a_i, b_i)$  represent the link distances in the X and Y directions respectively between the frames of the robot and the World Frame (WF) when the former is in it's home configuration, i.e., no joint is actuated.

The goal of this approach in this case study is to find the optimal combination of  $(a_i, b_i)$  in such a way to get the maximum rotation around a point in an enclosed environment.

From here, the forward kinematics that relates the WF to the tool tip  $A$  can be obtained using a classical transformation matrix  $T$  defined as follows:

$$T = \begin{bmatrix} \cos q_3 & -\sin q_3 & a_1 + a_2 + a_3 + q_1 + L \cos q_3 \\ \sin q_3 & \cos q_3 & b_1 + b_2 + b_3 + q_2 + L \sin q_3 \\ 0 & 0 & 1 \end{bmatrix} \quad (1)$$

Where  $q_1$ ,  $q_2$  and  $q_3$  represent the joint values of the stages in the X, Y and  $\theta$  directions respectively. For the purpose of SEM micromanipulation, the tool needs to be always directed towards the RCM, hence based on this assumption, the problem formulation can be reduced to 2 DoF resulting in the following kinematic model: the value of the  $\theta$  joint  $q_3$  is dependant on the value of the first two  $q_1$  and  $q_2$ :

$$q_3 = \arctan \frac{b_1 + b_2 + b_3 + q_2 - y_{rcm}}{a_1 + a_2 + a_3 + q_1 - x_{rcm}} \quad (2)$$

Where  $x_{rcm}$  and  $y_{rcm}$  represent the coordinates of the RCM regarding the robot WF.

From the direct model, an inverse kinematic model can be deduced which yields:

$$\begin{bmatrix} q_1 \\ q_2 \end{bmatrix} = \begin{bmatrix} x_p - a_1 - a_2 - a_3 - L \cos q_3 \\ y_p - b_1 - b_2 - b_3 - L \sin q_3 \end{bmatrix} \quad (3)$$

Where  $x_p$  and  $y_p$  represent the desired position of the tool tip  $A$ .

The original robot had six nanopositionners mounted in series, for the choice of the stages in this planar study, the one of the original robot were chosen as depicted in **Figure 4**

CLL42 (X stage):

- Size: 54.8 x 12 (mm)
- Maximum travel distance: 145.2 mm
- Size of the immobile part: 200x 10 mm

SLC-2490 (Y stage):

- Size: 90 x 6 mm
- Maximum travel distance: 63 mm
- Size of the immobile part: 90 x 10 mm

SR-5714 (theta stage):

- Size: 57 x 57 mm
- Travel distance: infinite



Fig. 5. Dimensions and maximum strokes of the micropositioning stages used in the study

The maximum stroke of each stage, as well as the dimension of the immobile and mobile parts are taken into consideration with the direct kinematic model to construct a geometrical planar motion model with regards to joint parameters. Since the main objective of this study is robot design in an enclosed space, all the parts of the geometrical model of the robot were defined as collision blocks.

## B. SEM Environment Definition

Regarding the SEM, our focus lies on the  $XOY$  plane within the interior environment, passing through the center of the fixed plate and of the SEM, as we aim to enhance rotations within this plane (**Figure 6**) to facilitate robotic tasks that require ample rotation around the  $Z$  axis. Another geometrical model was created based on it, which was referenced to the same WF as the 2D robotic model.

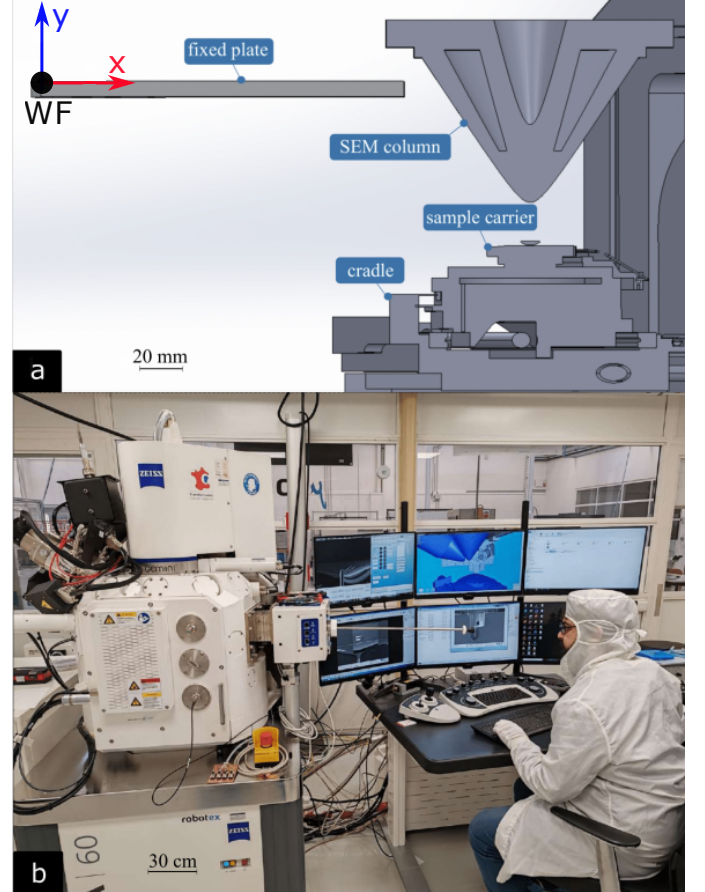


Fig. 6. Cross section of the SEM (a), outside view of the SEM next to a human operator (b)

In serial robotic systems, it is advisable to position the largest stage at the base, followed by progressively smaller stages toward the extremity. Where the base stage bears the entire mechanical load. It should be noted that the fixed plate in **Figure 6** refers to the frame that the robot is attached to.

**Figure 7** presents the result of the modelling process as the robot can be visualised inside the SEM with the tool directed towards the RCM. This is made possible by defining the models as collision blocks in the Robotics Systems Toolbox in MATLAB, and from this definition contact between the robot and the SEM environment can be detected.

## III. CONFIGURATION FREE SPACE ESTIMATION

To achieve robotic tasks at this scale, obtaining large rotations at this point of interest are of great importance, hence the following will introduce the method of calculating

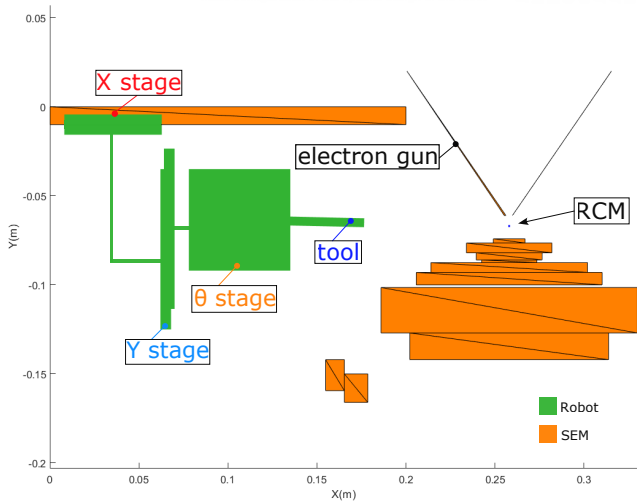


Fig. 7. Geometrical model representation of the robot inside the SEM using collision blocks

this angle of interest from a given robot design by estimating the configuration free space  $Q$  of the robot. The configuration free space calculation corresponds to the group containing all possible combinations of robot configuration  $(q_1, q_2, q_3)$  where no collision is detected.

Using analytical methods presented in the literature [14] or hierarchical approaches [15] would prove challenging considering the complex geometry of the environment. Instead we opted for a heuristic approach in varying the joint parameters using a step size of 2mm, which is suitable for a workspace estimation for robot at the scale of tens of centimeters. The configuration free space of a given robot design, i.e., the combination of  $q_1, q_2$  and  $q_3$  where no collision of the robot with itself or with the SEM environment occurs is quantified using this method.

From the configuration free space  $Q$ , we could identify the 2 configurations  $Q_{min}$  and  $Q_{max}$  that correspond to the maximum and minimum angle obtainable in the workspace, since  $q_3$  is the joint parameter representing the rotation of the  $\theta$  joint, the maximal angle can be expressed as

$$\varphi = Q_{max}(q_3) - Q_{min}(q_3) \quad (4)$$

Where  $\varphi$  corresponds to the objective function that is required to be maximized to ensure large rotations around the RCM.

For the simulations, an arbitrary tool of length 7 cm and width of 5mm was chosen. **Figure 8** presents the same robot design in the  $Q_{min}$  (green) and  $Q_{max}$  (blue) configurations.

#### IV. OPTIMIZATION PARAMETERS CALCULATION

After obtaining the method to calculate the objective function, finding the optimal design parameters (combination of  $a_i$  and  $b_i$ ) is the topic to be investigated in this section.

The nature of the objective function is implicit since the variables influencing it are resulting from a simulation. Meaning using popular optimization methods such

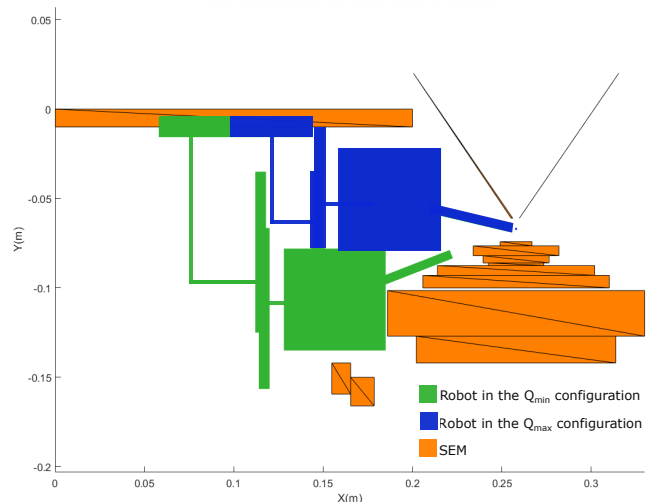


Fig. 8. Geometrical model illustrating the robot in  $Q_{min}$  and  $Q_{max}$  configurations

as stochastic gradient descent [16] and Adam [17] is not feasible.

Instead, a direct optimization method, the Hooke-Jeeves pattern search method is used in this study. In the robotics field, this method has been demonstrated in joint optimization [18]. It operates by iteratively exploring the design parameter search space (values of  $a_i$  and  $b_i$ ), adjusting step sizes and directions based on the objective function's evaluations. Starting with an initial guess, the algorithm performs exploratory moves by evaluating the objective function at the current point in the parameter space and searching along a pattern direction. If an improvement is found, the algorithm proceeds with a poll step, advancing further in the same direction; otherwise, it shrinks the step size and retries. In cases where the poll step fails to improve the objective, a coordinate search ensues, adjusting each coordinate independently to seek a better solution. This process iterates until the convergence of the design parameters is reached, i.e. the search direction becomes sufficiently small (0.1 mm) implying the finding of a local maximum in the objective function.

To avoid the problem of only finding the solution to the function locally in the stead of finding the global maximum of the function, numeral searches were conducted while varying the initial guess over the design parameter space[19].

The advantages of using this function include fast convergence (**Figure 9**), especially when compared to fine grid search method, which in this case would include 6 nested for loops. In the next section, the results of this method are going to be presented.

#### V. RESULTS

The optimization method resulted in the following design parameters that correspond to the optimal design of the robot according to the objective function that was set to align with the demands of robot dexterity for micromanipulation.

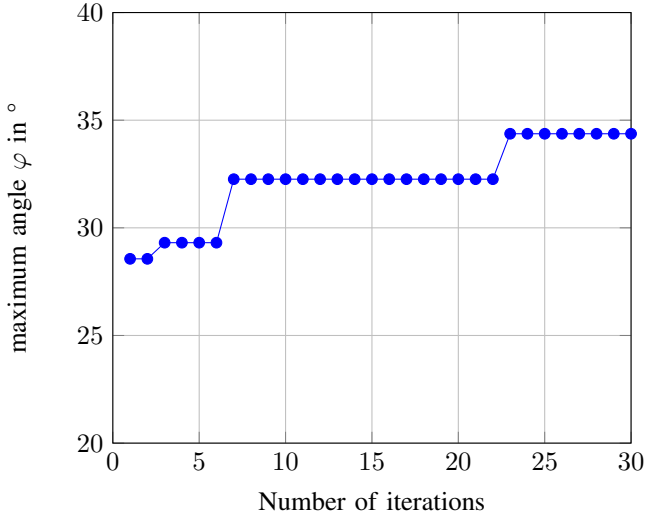


Fig. 9. Graph showing the convergence speed of the Hooke-Jeeves method

TABLE I  
OPTIMAL DESIGN PARAMETERS

$a_1$	$b_1$	$a_2$	$b_2$	$a_3$	$b_3$
2.74 cm	-1 cm	3.16 cm	-7 cm	3.95 cm	0.5 cm

The robot with these design parameters could achieve a rotation of  $34.37^\circ$  around the RCM. Which when compared to the current robot employed in the SEM that could rotate by  $14^\circ$ , proves the effectiveness of this method. Furthermore, it proved the importance of considering the work of the robot in the robotic architecture process.

To validate the feasibility of the results, we developed a rapidly exploring random tree (RRT) algorithm to check if it was possible for the robot to go from the configuration  $Q_{min}$  to  $Q_{max}$  without collision, it indeed resulted in the affirmation of the potentiality in reaching the two configurations as shown in **Figure 10**.

TABLE II

JOINT PARAMETERS FOR THE MINIMUM AND MAXIMUM ANGLE CONFIGURATIONS

	$q_1$	$q_2$	$q_3$
$Q_{min}$	89 mm	24.5 mm	$-13.1^\circ$
$Q_{max}$	59 mm	-31.5 mm	$21.27^\circ$

**Figure 11** illustrates the robot in its optimal design in a random configuration according to the set criteria.

## VI. CONCLUSION

This paper introduced an innovative approach for optimizing robot design within constrained environments. By leveraging a novel method to calculate free configuration space, we successfully derived an objective function aligning

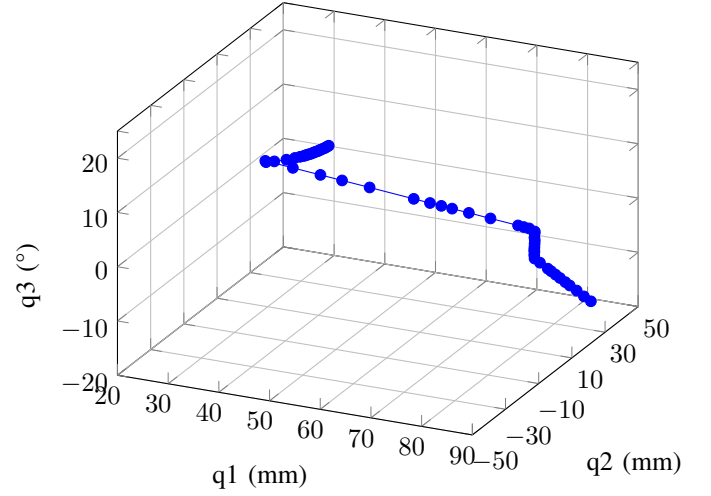


Fig. 10. Graph demonstrating using RRT algorithm for path planning going from configurations  $Q_{min}$  to  $Q_{max}$  without collision with the SEM systems

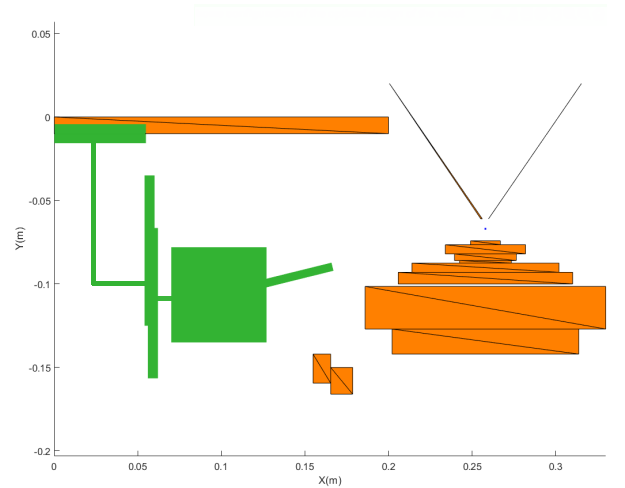


Fig. 11. Geometrical model expressing of the robot in its optimal design in a random configuration

with the key criteria of robot functionality. Subsequently, employing a direct optimization method enabled us to identify design parameters that maximize the rotation of the robot in a plane of interest to be more efficient in doing robotic tasks. We have demonstrated that the rotation angle can reach  $34^\circ$  for the considered study. The  $Q_{min}$  and  $Q_{max}$  can be reached without collision with the SEM using RRT algorithm for path planning

Moving forward, future endeavors will focus on expanding the objective function to incorporate multiple criteria and to push robotic architecture for SEM micromanipulation, as well as investigating innovative mechanisms to push the miniaturisation process forward to enable a more interesting workspace.

## VII. ACKNOWLEDGEMENT

This work has been partially funded by the DYN-ABOT Project under the contract ANR-21-CE10-0016, by

Région Bourgogne Franche-Comté, the EIPHI Graduate School (ANR-17-EURE-0002) and the French RENATECH and ROBOTEX networks (TIRREX ANR-21-ESRE-0015) through their FEMTO-ST technological facilities MIMENTO and CMNR. We thank Olivier Lehmann for his technical support for this work.

## REFERENCES

- [1] M. J. Lum, J. Rosen, M. N. Sinanan, and B. Hannaford, "Kinematic optimization of a spherical mechanism for a minimally invasive surgical robot," in *IEEE International Conference on Robotics and Automation, 2004.*, vol. 1. IEEE, 2004, pp. 829–834.
- [2] R. Saravanan, S. Ramabalan, N. G. R. Ebenezer, and C. Dharmaraja, "Evolutionary multi criteria design optimization of robot grippers," *Applied Soft Computing*, vol. 9, no. 1, pp. 159–172, 2009.
- [3] M. Bugday and M. Karali, "Design optimization of industrial robot arm to minimize redundant weight," *Engineering Science and Technology, an International Journal*, vol. 22, no. 1, pp. 346–352, 2019.
- [4] P. K. Jamwal, S. Xie, and K. C. Aw, "Kinematic design optimization of a parallel ankle rehabilitation robot using modified genetic algorithm," *Robotics and Autonomous Systems*, vol. 57, no. 10, pp. 1018–1027, 2009.
- [5] J.-T. Lin, C. Girerd, J. Yan, J. T. Hwang, and T. K. Morimoto, "A generalized framework for concentric tube robot design using gradient-based optimization," *IEEE Transactions on Robotics*, vol. 38, no. 6, pp. 3774–3791, 2022.
- [6] S. Zeghloul and J. Pamanes-Garcia, "Multi-criteria optimal placement of robots in constrained environments," *Robotica*, vol. 11, no. 2, p. 105–110, 1993.
- [7] M. R. Ahmad, M. Nakajima, S. Kojima, M. Homma, and T. Fukuda, "In situ single cell mechanics characterization of yeast cells using nanoneedles inside environmental sem," *IEEE Transactions on Nanotechnology*, vol. 7, no. 5, 2008.
- [8] C. Ru, Y. Zhang, Y. Sun, Y. Zhong, X. Sun, D. Hoyle, and I. Cotton, "Automated four-point probe measurement of nanowires inside a scanning electron microscope," *IEEE Transactions on Nanotechnology*, vol. 10, no. 4, pp. 674–681, 2010.
- [9] R. R. Kumar, S. Hassan, O. S. Sukas, V. Eichhorn, F. Krohs, S. Fatikow, and P. Boggild, "Nanobits: customizable scanning probe tips," *Nanotechnology*, vol. 20, no. 39, p. 395703, 2009.
- [10] J.-Y. Rauch, O. Lehmann, P. Rougeot, J. Abadie, J. Agnus, M. Suarez, et al., "Smallest microhouse in the world, assembled on the facet of an optical fiber by origami and welded in the  $\mu$ robotex nanofactory," *Journal of Vacuum Science & Technology A*, vol. 36, no. 4, 2018.
- [11] R. Hannouch, G. Colas, J.-Y. Rauch, V. Reynaud, J. Agnus, O. Lehmann, F. Marionnet, and C. Clévy, "Robotic-based selection, manipulation and characterization of 3d microscale particles with complex structures in sem," in *International Conference on Manipulation, Automation and Robotics at Small Scales*. IEEE, 2023, pp. 1–6.
- [12] Y. Lei, C. Clévy, J.-Y. Rauch, and P. Lutz, "Large-workspace polyarticulated micro-structures based-on folded silica for tethered nanorobotics," *IEEE Robotics and Automation Letters*, vol. 7, no. 1, pp. 88–95, 2021.
- [13] A. Benouhiba, L. Wurtz, J.-Y. Rauch, J. Agnus, K. Rabenorosa, and C. Clévy, "Nanorobotic structures with embedded actuation via ion induced folding," *Advanced Materials*, vol. 33, no. 45, p. 2103371, 2021.
- [14] K. Sun and V. J. Lumelsky, "A topological study of robot free configuration space," *IEEE/RSJ International Workshop on Intelligent Robots and Systems*, pp. 575–580 vol.2, 1991.
- [15] J. Yang, P. Dymond, and M. Jenkin, "Hierarchical probabilistic estimation of robot reachable workspace," in *Proceedings of the 6th International Conference on Informatics in Control, Automation and Robotics - Volume 1*, 2009, pp. 60–66.
- [16] F. Piltan and S. T. Haghghi, "Design gradient descent optimal sliding mode control of continuum robots," *IAES International Journal of Robotics and Automation*, vol. 1, no. 4, p. 175, 2012.
- [17] D. O. Melinte and L. Vladareanu, "Facial expressions recognition for human–robot interaction using deep convolutional neural networks with rectified adam optimizer," *Sensors*, vol. 20, no. 8, p. 2393, 2020.
- [18] S. Ha, S. Coros, A. Alspach, J. Kim, and K. Yamane, "Joint optimization of robot design and motion parameters using the implicit function theorem," in *Robotics: Science and systems*, vol. 13, 2017, pp. 10–15 607.
- [19] B. Kryzhanovsky, B. Magomedov, and A. Fonarev, "On the probability of finding local minima in optimization problems," in *IEEE International Joint Conference on Neural Network*, 2006, pp. 3243–3248.